Photoelectrochemistry

Deutsche Ausgabe: DOI: 10.1002/ange.201504427
Internationale Ausgabe: DOI: 10.1002/anie.201504427

Hematite-Based Solar Water Splitting in Acidic Solutions: Functionalization by Mono- and Multilayers of Iridium Oxygen-Evolution Catalysts**

Wei Li, Stafford W. Sheehan, Da He, Yumin He, Xiahui Yao, Ronald L. Grimm, Gary W. Brudvig, and Dunwei Wang**

Abstract: *Solar water splitting in acidic solutions has important technological implications, but has not been demonstrated to date in a dual absorber photoelectrochemical cell. The lack of functionally stable water-oxidation catalysts (WOCs) in acids is a key reason for this slow development. The only WOCs that are stable at low pH are Ir-based systems, which are typically too expensive to be implemented broadly. It is now shown that this deficiency may be corrected by applying an ultra-thin monolayer of a molecular Ir WOC to hematite for solar water splitting in acidic solutions. The turn-on voltage is observed to shift cathodically by 250 mV upon the application of a monolayer of the molecular Ir WOC. When the molecular WOC is replaced by a heterogeneous multilayer derivative, stable solar water splitting for over 5 h is achieved with near-unity Faradaic efficiency.*

To meet rapidly rising energy demand without devastating the environment, we need a new energy scheme where renewable sources will play a key role.[1] Of many chemical candidates for this new energy infrastructure, H_2 produced by H_2O splitting holds great promise owing to its high energy density per kilogram and potential ease of transportation and utilization. Generating H_2 from H_2O is also appealing for thermodynamic reasons: The energetics required match those of the solar spectrum well.[2] How to carry out the constituent oxidation and reduction half-reactions efficiently at a reasonable cost, however, remains a challenge.[3] To date, the most efficient approaches reported either involve or are entirely powered by photovoltaic modules.[4–6] The comparatively simpler approach of direct water photolysis (also known as photoelectrochemistry, PEC) suffers from low efficiency, poor durability, or both.[7] Poor integration of catalysts with photoelectrodes is one important reason for this slow development.[8] Taking the photoanode as an example,[9–13] on a system level, its operation needs to be matched with a photocathode. Because the only commercially successful membranes to separate the photoanode and photocathode are proton exchange membranes, PEC H_2O oxidation in acidic solutions deserves particular attention.[14] While catalysts for H_2O reduction in acidic solutions are readily available, those for H_2O oxidation at low pH are rare,[15,16] with Ir-based systems being the only functionally stable examples.[17–19] One criticism that Ir-based catalysts have to address is the cost associated with the scarcity of the element in the earth's crust; a solution to this problem is made possible by a recently developed strategy that utilizes monolayers of a molecular heterogenized catalyst that can be derived from its homogeneous analogue.[20–24] Herein we show that the same strategy can be readily applied to enable the first example of hematite-based complete water splitting in acidic solutions.

As has been recently reported by some of the co-authors (Sheehan and Brudvig)[21] and represented in Figure 1a, the molecular identity of our heterogenized Ir water oxidation catalyst (het-WOC) is preserved by its bidentate ligands, whereas strong direct binding of the Ir centers to the photoelectrode corrects the drawback of poor stability often found with molecular catalysts. The molecular nature of the Ir het-WOC distinguishes itself from the more widely studied IrO_2 nanoparticles that have been previously integrated with hematite.[36] The effect of the het-WOC on hematite[25] PEC performance is evident in Figure 1b, where the turn-on voltages (V_{on}) are cathodically shifted by 0.25 V (from 0.85 V to 0.60 V using the Butler method; see the Supporting Information, Figure S1, for more details) at pH 1.01. To show that the observed performance enhancement was indeed a result of Ir het-WOC decoration, we examined the photo-

[*] W. Li, D. He, Y. He, X. Yao, Prof. Dr. D. Wang
Department of Chemistry, Merkert Chemistry Center, Boston College
2609 Beacon St., Chestnut Hill, MA 02467 (USA)
E-mail: dunwei.wang@bc.edu
S. W. Sheehan, Prof. Dr. G. W. Brudvig
Department of Chemistry, Yale University
225 Prospect Street, PO Box 208107, New Haven, CT 06520-8107 (USA)
E-mail: gary.brudvig@yale.edu
Prof. Dr. R. L. Grimm
Department of Chemistry and Biochemistry
Worcester Polytechnic Institute
100 Institute Road, Worcester, MA 01609 (USA)

[**] The work at BC was funded by the NSF (DMR 1055762), and the work carried out at Yale was funded by the Argonne-Northwestern Solar Energy Research (ANSER) Energy Frontier Research Center funded by the U.S. Department of Energy (DE-SC0001059, G.W.B.), an NSF Graduate Research Fellowship (DGE 1122492, S.W.S.), and the Yale Entrepreneurial Institute (research materials, S.W.S.). We are grateful for the a-Si photocathode material from Prof. Ali Javey's group at UC Berkeley and technical support by S. Shepard, L.-Y. Chou, and C.-K. Tsung at BC. US Patent Application Number 14/317,906 by S.W.S. and G.W.B. contains intellectual property described in this article. The other authors declare no competing financial interest.

Supporting information for this article is available on the WWW under http://dx.doi.org/10.1002/anie.201504427.

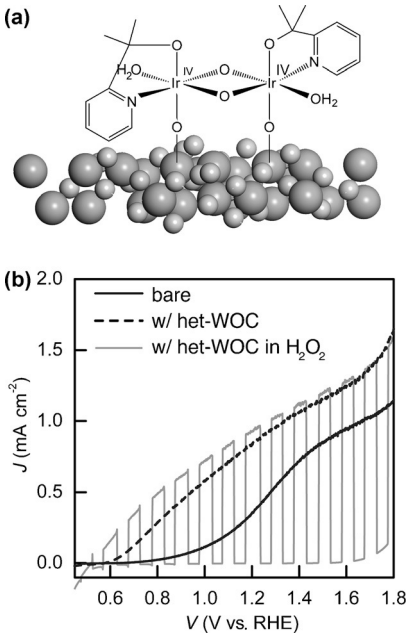

Figure 1. Application of a monolayer of the molecular Ir WOC on hematite. a) Representation of the proposed WOC molecular structure on a hematite surface. The surface binding is made possible by Ir-O-Fe bonding. b) Polarization curves of hematite photoanodes with (-----) and without Ir WOC (——). The electrolyte was 0.1 M KNO_3 (pH 1.01, adjusted by HNO_3), and lighting was AM 1.5 at 100 mW cm^{-2}. The polarization curve measured in the presence of H_2O_2 is included (gray; under chopped lighting conditions) for comparison. The scan directions for all curves are from positive to negative.

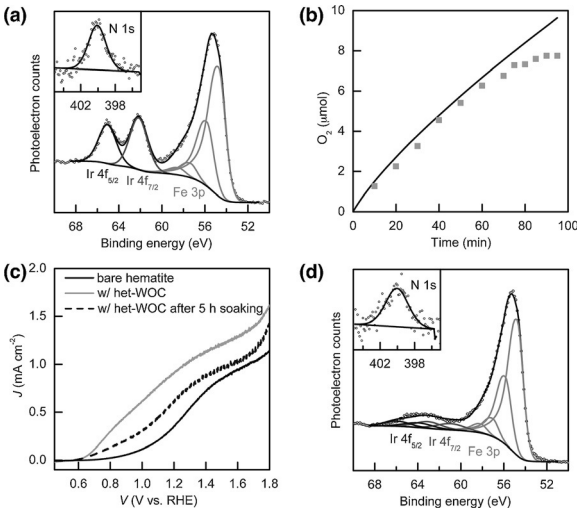

Figure 2. Surface studies of the het-WOC-decorated hematite photoelectrode. a) X-ray photoelectron spectroscopy analysis confirming the attachment of Ir and bidentate pyalc ligand. Inset: the spectrum and its fitting corresponding to N 1s binding energies. b) Detection of evolved O_2 by het-WOC-decorated hematite. Electrolyte: 0.1 M KNO_3 (pH adjusted to 1.01); lighting condition: AM 1.5 illumination at 100 mW cm^{-2}; applied potential: 1.23 V vs. RHE. Black trace: theoretical amount based on passed charge. c) Polarization curves of various photoelectrodes. Test conditions were identical to those in panel (b). d) XPS spectra after a 10 h stability test. Inset: the spectrum of N 1s binding energies.

electrode using X-ray photoelectron spectroscopy (XPS). Survey scans (Supporting Information, Figure S3) revealed that the only elements present are Fe, O, C, Ir, and N. The peaks at 65 eV and 62 eV correspond to Ir $4f_{5/2}$ and Ir $4f_{7/2}$, respectively (Figure 2a). The binding energies agree well with those for Ir^{IV} in the surface-bound species, as supported by previous studies on this system.[21] The inset in Figure 2a confirms the existence of N 1s, which is most likely due to the pyalc ligand, which is critical to maintaining the molecular identity of the Ir WOC. The ratio of Ir^{IV} to pyalc was calculated as ca. 1:1, in good agreement with what is expected from the het-WOC structure shown in Figure 1a.

It is noted that, although corrosion of hematite in acidic solutions is known, the reactions are non-redox in nature and hence are not expected to contribute to photocurrents. Furthermore, the reactions are slow enough to permit PEC characterization of bare hematite photoelectrodes (Supporting Information, Figure S5). Important to our discussions, the steady-state current voltage curves of het-WOC-decorated hematite without sacrificial hole scavengers are comparable to those with hole scavengers (gray curve in Figure 1b, where H_2O_2 is present) in terms of V_{on} and saturation current densities, strongly supporting that the excellent water-oxidation catalytic activities are due to the Ir het-WOC.[21] To experimentally verify that the measured photocurrents are indeed a result of water oxidation, we measured the evolved O_2 using a Clark-type oxygen sensor (Figure 2b), where 1.23 V vs. RHE (reversible hydrogen electrode) was applied to the hematite/het-WOC photoelectrode.[26] The calculated Faradaic efficiency was 94% during the first 50 min. The efficiency started to decrease after 60 min, however, and the amount of O_2 leveled off after 80 min. Several reasons may help explain the observation. First, the detection is based on dissolved O_2. Saturation of O_2 in the solution could lead to apparent deviations of the charge/O_2 linear dependence as shown in Figure 2b. Because of the large volume of solutions used here, our calculations show that this cause is unlikely (see the Supporting Information). Second, the Ir het-WOC may be stripped off the photoelectrode during measurements by oxidation of its ligands or simple corrosion of the underlying hematite in highly acidic solutions. To test the latter case, we found that by simply soaking the het-WOC decorated hematite in testing solutions without passing through any charge, a dramatic degradation of the PEC performance in the form of an anodic shift (Figure 2c) was observed. XPS studies showed that, although peaks corresponding to the Ir het-WOC are still observable after 10 h of electrolysis, the intensities are obviously decreased (Figure 2d). Given that the monolayer catalyst does not provide a compact, high-density coverage of the hematite surface, it is reasonable that acids corrode hematite to undermine the attachment of het-WOC to hematite. It is, therefore, concluded that significant loss of surface-attached Ir het-WOC during electrolysis indeed took place. When het-WOC dissolves in H_2O, it may serve as a redox shuttle between the anode and cathode, contributing to the photocurrent but not O_2 evolution. To further verify this hypothesis, we reloaded het-WOC on hematite after 10 h of stability testing,

replaced the test solution, and observed full recovery of the PEC performance (Supporting Information, Figure S6). The results support that the photoelectrode degradation is due to the detachment of the het-WOC from the hematite photoelectrode. It is noted that because the excellent stability of the Ir het-WOC under oxidation conditions has been demonstrated previously,[21] the catalyst detachment is most likely caused by corrosion of hematite rather than ligand loss, as supported by XPS (Figure 2).

Several important advantages are offered by the ultra-thin monolayer of het-WOC. For example, it significantly reduces the amount of catalyst needed to achieve desired performance, and imparts limited corrosion resistance. That a single-layer catalyst readily shifts V_{on} by as much as 250 mV speaks of the paramount importance of controlling the photoelectrode/electrolyte interface of a PEC.[19,26–30] Moreover, the thin layer absorbs little light, making it highly versatile in integration with various types of photoelectrode materials (Supporting Information, Figure S8). By comparison, the more extensively studied WOCs such as Co-P_i or amorphous $NiFeO_x$ compete with the photoelectrode for light absorption to a certain extent;[31,32] aside from that, they do not function in acidic solutions. These benefits notwithstanding, the instability of the het-WOC-decorated hematite over the course of hours presents a critical challenge. We envision that replacing the hematite/het-WOC interface with an acid-stable material such as WO_3 should help improve the stability. Approaches toward this direction are under development.

To further study what is enabled by an acid-active WOC, we next pursued complete solar water splitting with a bulk heterogeneous derivative of a {Cp*Ir} precatalyst (Cp* = pentamethylcyclopentadienyl), the "blue-layer" IrO_x WOC.[18,33,34] Our rationale was that this amorphous IrO_x WOC resulting from anodic photoelectrodeposition provides a more dense coverage on the hematite surface to prevent solution penetration. The expectation was confirmed by transmission electron microscopy (TEM, Figure 3a), which was obtained by a brief (10 s) deposition at 2.5 V (vs. SCE, saturated calomel electrode; see the Supporting Information).

As far as PEC performance is concerned, the IrO_x WOC yielded comparable results on the surface of hematite as the Ir het-WOC (Figure 3b; see the Supporting Information, Figure S9 for side-by-side comparison). A similarly low V_{on} of 0.6 V was obtained. Comparing the steady-state current–voltage curve with that in the presence of the hole scavenger H_2O_2 (Figure 3c), we see that the photocurrent is limited by the light-harvesting and charge-separation capabilities of hematite, but not the charge transfer through the catalyst. The result further highlights the outstanding H_2O-oxidation activity of the IrO_x WOC. Open-circuit voltage measurements in dark and light for bare hematite, with het-WOC, and with IrO_x WOC revealed that the IrO_x clearly shifts the dark equilibrium potential (1.1 V) close to the water oxidation potential of 1.23 V (Supporting Information, Figure S12). In the absence of surface states, the dark equilibrium potential is expected to align with the water oxidation potential; any mismatch is perceived as an undesired potential drop in the Helmholtz layer that does not contribute to charge separation in the photoelectrode.[26] The result suggests that the IrO_x improves the PEC performance by changing the interface energetics. Its application increases the degree of band bending within the photoelectrode, affording better charge separation. The effect of het-WOC, however, is less clear. The dark equilibrium potential (0.9 V) only represents a modest shift of 0.1 V when compared with bare hematite (0.8 V). Although it is reasonable to expect the shift to be modest because the het-WOC provides less complete coverage of the hematite surface than IrO_x and, hence, does not modify the surface energetics as significantly as IrO_x, the magnitude fails to explain the observed PEC performance improvement. We suspect that much improved kinetics may play an important role here, as the het-WOC has been shown to outperform IrO_x under certain electrocatalytic conditions.[21] Further studies are thus needed to better understand this system.

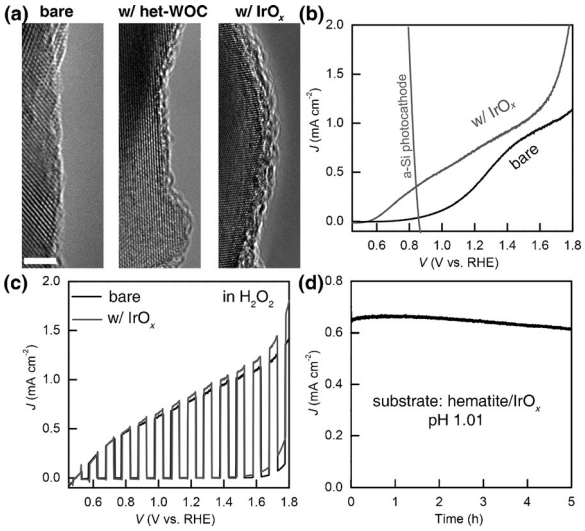

Figure 3. Structural and photoelectrochemical studies of IrO_x "blue layer" decorated hematite photoanode. a) Transmission electron micrographs showing the morphologies of bare hematite (left), with het-WOC (middle), and with a thin IrO_x "blue layer" (right). Scale bar: 2 nm. (b) Polarization curves showing the PEC behavior of IrO_x-decorated hematite tested in 0.1 M KNO_3 (pH 1.01) under AM 1.5 illumination. The polarization curve of a matching amorphous Si (a-Si) photocathode is shown as a gray trace. c) Polarization curves measured in the presence of H_2O_2 under chopped illumination. d) Chronoamperometry showing the stability of hematite/IrO_x over 5 h with only a 5% decrease.

Most important to our next discussions, the stability of the photoelectrode in acids is now greatly improved, with only a 5% decay over 5 h of electrolysis run at 1.23 V vs. RHE (Figure 3d; 0.66 mA cm^{-2} at $t = 0$ and 0.61 mA cm^{-2} at $t =$ 5 h). The outstanding stability opens up new doors to constructing devices for unassisted water splitting, with amorphous Si (a-Si) as a photocathode.[25,35] The typical current–voltage performance of the a-Si photocathode is shown in Figure 3b as a gray trace. It overlaps with the photoanode curve with IrO_x present, and the current density at the cross-point is 0.36 mA cm^{-2}. With simulated sunlight passing through the photoanode (including the IrO_x), a significant reduction in the light intensity is expected, even

beyond the absorption of hematite, owing to IrO_x absorption and light scattering (Supporting Information, Figure S14). As such, the measured photocurrents represent the lower bound of what can be achieved by the hematite/a-Si system. Even with these constraints, it is highly encouraging to measure meaningful photocurrents without applying an external bias in highly acidic solutions. The production of O_2 and H_2 was detected using a Clark-type electrode and mass spectrometry, respectively (Figure 4). Within the first 90 min, near 100 %

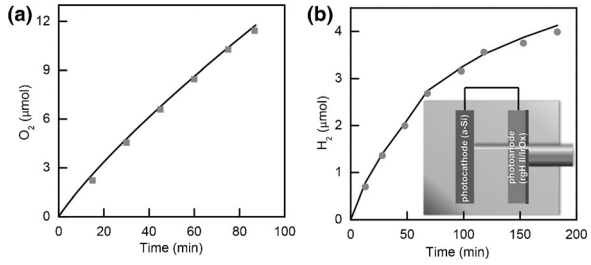

Figure 4. Product detection for photoanode (IrO_x-decorated hematite) and photocathode (a-Si) in acidic solutions (pH 1.01). a) Amount of evolved O_2 by detected by a Clark-type oxygen sensor. Black line: theoretical O_2 amount calculated from charges. b) H_2 generated in unassisted overall water splitting system detected by mass spectrometry without external bias. The tandem device configuration is represented in the inset.

Faradaic efficiency was measured for O_2 production, beyond which the solution would be saturated and further detection is not possible. Similarly, the Faradaic efficiency for H_2 generation was close to 100 % during the first 3 h of testing. It is noted that the a-Si photocathode stability in highly acidic solutions requires further optimization because its TiO_2 protection layer is etched relatively rapidly. To the best of our knowledge, this is the first unassisted solar water splitting with a meaningful efficiency (estimated efficiency 0.44 %) that has been obtained under acidic conditions.

To realize the full potential of solar water splitting as a large-scale energy storage solution, we need a photoanode and a photocathode with complementary light absorption and matching performance under the same operation conditions (for example, pH). With this consideration in mind, we see that the lack of functional H_2O oxidation catalysts at low pH presents a conspicuous challenge. Ir-free WOCs that work for extended period of time in acid solutions have not been reported. As such, our strategy of utilizing an ultrathin, monolayer Ir WOC derived from a molecular analogue is particularly meaningful as it provides a temporary solution to the issues connected to the high cost of Ir by minimizing the amount catalyst used. That the catalyst enables high performance of hematite at low pH is encouraging. Although significant work is still needed to further stabilize the het-WOC/hematite combination, we show that in principle the design should work by employing a heterogeneous coverage of IrO_x derived from an organometallic Ir species. To the best of our knowledge, this is the first time complete solar water splitting in acidic solutions by hematite, or any other photoanode, has been achieved.

Keywords: hematite · homogeneous catalysis · iridium · photoelectrochemistry · solar water splitting

How to cite: *Angew. Chem. Int. Ed.* **2015**, *54*, 11428–11432
Angew. Chem. **2015**, *127*, 11590–11594

[1] N. S. Lewis, *Science* **2007**, *315*, 798–801.
[2] J. R. Bolton, S. J. Strickler, J. S. Connolly, *Nature* **1985**, *316*, 495–500.
[3] R. E. Blankenship, D. M. Tiede, J. Barber, G. W. Brudvig, G. Fleming, M. Ghirardi, M. R. Gunner, W. Junge, D. M. Kramer, A. Melis, T. A. Moore, C. C. Moser, D. G. Nocera, A. J. Nozik, D. R. Ort, W. W. Parson, R. C. Prince, R. T. Sayre, *Science* **2011**, *332*, 805–809.
[4] O. Khaselev, J. A. Turner, *Science* **1998**, *280*, 425–427.
[5] S. Y. Reece, J. A. Hamel, K. Sung, T. D. Jarvi, A. J. Esswein, J. J. H. Pijpers, D. G. Nocera, *Science* **2011**, *334*, 645–648.
[6] J. Luo, J.-H. Im, M. T. Mayer, M. Schreier, M. K. Nazeeruddin, N.-G. Park, S. D. Tilley, H. J. Fan, M. Grätzel, *Science* **2014**, *345*, 1593–1596.
[7] A. Fujishima, K. Honda, *Nature* **1972**, *238*, 37–38.
[8] B. Klahr, S. Gimenez, F. Fabregat-Santiago, J. Bisquert, T. W. Hamann, *J. Am. Chem. Soc.* **2012**, *134*, 16693–16700.
[9] Y. Lin, S. Zhou, S. W. Sheehan, D. Wang, *J. Am. Chem. Soc.* **2011**, *133*, 2398–2401.
[10] M. T. Mayer, C. Du, D. Wang, *J. Am. Chem. Soc.* **2012**, *134*, 12406–12409.
[11] R. S. Selinsky, S. Shin, M. A. Lukowski, S. Jin, *J. Phys. Chem. Lett.* **2012**, *3*, 1649–1656.
[12] R. Franking, L. Li, M. A. Lukowski, F. Meng, Y. Tan, R. J. Hamers, S. Jin, *Energy Environ. Sci.* **2013**, *6*, 500–512.
[13] J. Wu, W. Walukiewicz, K. M. Yu, J. W. Ager, E. E. Haller, H. Lu, W. J. Schaff, Y. Saito, Y. Nanishi, *Appl. Phys. Lett.* **2002**, *80*, 3967–3969.
[14] S. Haussener, C. Xiang, J. M. Spurgeon, S. Ardo, N. S. Lewis, A. Z. Weber, *Energy Environ. Sci.* **2012**, *5*, 9922–9935.
[15] Y. V. Geletii, B. Botar, P. Kögerler, D. A. Hillesheim, D. G. Musaev, C. L. Hill, *Angew. Chem. Int. Ed.* **2008**, *47*, 3896–3899; *Angew. Chem.* **2008**, *120*, 3960–3963.
[16] Y. V. Geletii, C. Besson, Y. Hou, Q. Yin, D. G. Musaev, D. Quiñonero, R. Cao, K. I. Hardcastle, A. Proust, P. Kögerler, C. L. Hill, *J. Am. Chem. Soc.* **2009**, *131*, 17360–17370.
[17] J. M. Spurgeon, J. M. Velazquez, M. T. McDowell, *Phys. Chem. Chem. Phys.* **2014**, *16*, 3623–3631.
[18] J. D. Blakemore, N. D. Schley, G. W. Olack, C. D. Incarvito, G. W. Brudvig, R. H. Crabtree, *Chem. Sci.* **2011**, *2*, 94–98.
[19] L. Badia-Bou, E. Mas-Marza, P. Rodenas, E. M. Barea, F. Fabregat-Santiago, S. Gimenez, E. Peris, J. Bisquert, *J. Phys. Chem. C* **2013**, *117*, 3826–3833.
[20] J. M. Thomsen, S. W. Sheehan, S. M. Hashmi, J. Campos, U. Hintermair, R. H. Crabtree, G. W. Brudvig, *J. Am. Chem. Soc.* **2014**, *136*, 13826–13834.
[21] S. W. Sheehan, J. M. Thomsen, U. Hintermair, R. H. Crabtree, G. W. Brudvig, C. A. Schmuttenmaer, *Nat. Commun.* **2015**, *6*, 6469.
[22] A. K. Vannucci, L. Alibabaei, M. D. Losego, J. J. Concepcion, B. Kalanyan, G. N. Parsons, T. J. Meyer, *Proc. Natl. Acad. Sci. USA* **2013**, *110*, 20918–20922.
[23] U. Hintermair, S. W. Sheehan, A. R. Parent, D. H. Ess, D. T. Richens, P. H. Vaccaro, G. W. Brudvig, R. H. Crabtree, *J. Am. Chem. Soc.* **2013**, *135*, 10837–10851.
[24] H. Dau, C. Limberg, T. Reier, M. Risch, S. Roggan, P. Strasser, *ChemCatChem* **2010**, *2*, 724–761.
[25] J. W. Jang, C. Du, Y. Ye, Y. Lin, X. Yao, J. Thorne, E. Liu, G. McMahon, J. Zhu, A. Javey, J. Guo, D. Wang, *Nat. Commun.* **2015**, *6*, 7447.

[26] C. Du, X. Yang, M. T. Mayer, H. Hoyt, J. Xie, G. McMahon, G. Bischoping, D. Wang, *Angew. Chem. Int. Ed.* **2013**, *52*, 12692 – 12695; *Angew. Chem.* **2013**, *125*, 12924 – 12927.
[27] C. Du, M. Zhang, J.-W. Jang, Y. Liu, G.-Y. Liu, D. Wang, *J. Phys. Chem. C* **2014**, *118*, 17054 – 17059.
[28] X. Yang, C. Du, R. Liu, J. Xie, D. Wang, *J. Catal.* **2013**, *304*, 86 – 91.
[29] M. T. Mayer, Y. Lin, G. Yuan, D. Wang, *Acc. Chem. Res.* **2013**, *46*, 1558 – 1566.
[30] Y. Lin, Y. Xu, M. T. Mayer, Z. I. Simpson, G. McMahon, S. Zhou, D. Wang, *J. Am. Chem. Soc.* **2012**, *134*, 5508 – 5511.
[31] R. D. L. Smith, M. S. Prévot, R. D. Fagan, Z. Zhang, P. A. Sedach, M. K. J. Siu, S. Trudel, C. P. Berlinguette, *Science* **2013**, *340*, 60 – 63.
[32] D. K. Zhong, M. Cornuz, K. Sivula, M. Gratzel, D. R. Gamelin, *Energy Environ. Sci.* **2011**, *4*, 1759 – 1764.
[33] J. D. Blakemore, N. D. Schley, M. N. Kushner-Lenhoff, A. M. Winter, F. D'Souza, R. H. Crabtree, G. W. Brudvig, *Inorg. Chem.* **2012**, *51*, 7749 – 7763.
[34] J. Huang, J. D. Blakemore, D. Fazi, O. Kokhan, N. D. Schley, R. H. Crabtree, G. W. Brudvig, D. M. Tiede, *Phys. Chem. Chem. Phys.* **2014**, *16*, 1814 – 1819.
[35] Y. Lin, C. Battaglia, M. Boccard, M. Hettick, Z. Yu, C. Ballif, J. W. Ager, A. Javey, *Nano Lett.* **2013**, *13*, 5615 – 5618.
[36] S. D. Tilley, M. Cornuz, K. Sivula, M. Grätzel, *Angew. Chem. Int. Ed.* **2010**, *49*, 6405 – 6408; *Angew. Chem.* **2010**, *122*, 6549 – 6552.

Received: May 15, 2015
Published online: July 14, 2015

